Mathematical Biosciences and Engineering

Research article

Global stability of a continuous bioreactor model under persistent variation of the dilution rate

Alejandro Rincón[1,2], Fredy E. Hoyos[3,*] and Gloria Restrepo[2]

[1] Grupo de Investigación en Desarrollos Tecnológicos y Ambientales (GIDTA), Facultad de Ingeniería y Arquitectura, Universidad Católica de Manizales, Carrera 23 N. 60–63, Manizales 170002, Colombia

[2] Grupo de Investigación en Microbiología y Biotecnología Agroindustrial (GIMIBAG), Instituto de Investigación en Microbiología y Biotecnología Agroindustrial, Universidad Católica de Manizales, Carrera 23 N. 60–63, Manizales 170002, Colombia

[3] Departamento de Energía Eléctrica y Automática, Facultad de Minas, Universidad Nacional de Colombia, Sede Medellín, Carrera 80 No. 65–223, Campus Robledo, Medellín 050041, Colombia

* **Correspondence:** Email: fehoyosve@unal.edu.co; Tel: +574309000.

Abstract: In this work, the global stability of a continuous bioreactor model is studied, with the concentrations of biomass and substrate as state variables, a general non-monotonic function of substrate concentration for the specific growth rate, and constant inlet substrate concentration. Also, the dilution rate is time varying but bounded, thus leading to state convergence to a compact set instead of an equilibrium point. Based on the Lyapunov function theory with dead-zone modification, the convergence of the substrate and biomass concentrations is studied. The main contributions with respect to closely related studies are: i) The convergence regions of the substrate and biomass concentrations are determined as function of the variation region of the dilution rate (D) and the global convergence to these compact sets is proved, considering monotonic and non-monotonic growth functions separately; ii) several improvements are proposed in the stability analysis, including the definition of a new dead zone Lyapunov function and the properties of its gradient. These improvements allow proving convergence of substrate and biomass concentrations to their compact sets, while tackling the interwoven and nonlinear nature of the dynamics of biomass and substrate concentrations, the non-monotonic nature of the specific growth rate, and the time-varying nature of the dilution rate. The proposed modifications are a basis for further global stability analysis of bioreactor models exhibiting convergence to a compact set instead of an equilibrium point. Finally, the

theoretical results are illustrated through numerical simulation, showing the convergence of the states under varying dilution rate.

1. Introduction

Continuous tank bioreactors are useful for producing chemical compounds, cultivating biomass, and for biological wastewater treatment [1–3]. In these bioreactors, the dilution rate and inlet substrate concentration have an important effect on the behavior of the biomass and substrate concentrations. Also, an overlarge dilution rate or equivalently low hydraulic retention time leads to biomass washout in most cases [4–7]. Adequate operation conditions of continuous bioreactors with avoidance of biomass washout can be studied through global and local stability analysis [3,7,8]. It has been found that in the chemostat model with non-monotonic growth function, two stable biomass equilibria may occur for certain values of the dilution rate, corresponding to biomass washout and to positive biomass. The initial condition determines which equilibrium is reached [3,7]. Some examples are the model for phenol and p-cresol mixture degradation in a continuously stirred tank bioreactor [9]; the microalgae Droop model [10]; the model for microalgae culture in presence of nitrifying bacteria [11]; the model of anaerobic digester [12]. In addition, if the yield coefficient is a function of the substrate concentration, a stable limit cycle exists for a certain range of the dilution rate, what is consistent with experimental results. Bioreactor operation with these limit cycles is usually avoided in practice [13–15].

Local stability can be studied by the indirect Lyapunov method, the main results include equilibrium points related to biomass existence and biomass washout, and the effect of dilution rate and inlet substrate concentration on the existence and stability of equilibria [7,16,17]. In contrast, global stability for constant dilution rate can be assessed by Lyapunov function theory, and the main results include the determination of global stability of the equilibrium associated with positive biomass concentration [9,11,18,19], stability of the equilibrium associated to biomass extinction [9,19,20], effect of kinetic parameters on the stability of equilibria [20], convergence of the additive combination of biomass, substrate and product concentrations [9,19]; domain of attraction of stable equilibria (see [11]); range of the input substrate concentration for global stability of the positive equilibrium point [21].

Some of these works are discussed at what follows. In [19], the global stability of a chemostat with overflow metabolism is studied. The state variables of the model are the concentrations of biomass, substrate, and by-product. The by-product secretion has an inhibitory effect on the growth of microorganisms, whereas the by-product excretion rate function is non-smooth. The existence and global stability of the equilibrium corresponding to positive biomass are proved, and the parameter conditions related to the existence of by-product are determined. In [9], the local and global stability of a model for phenol and cresol mixture degradation in a continuously stirred bioreactor is studied. The state variables are the concentrations of biomass, phenol and cresol. The biomass-specific growth rate involves inhibition caused by the substrate concentrations. The local asymptotic stability of the equilibrium point and the existence of local bifurcation in dependence on the dilution rate (D) are studied. It was found that two positive biomass equilibria exist, and the interval of D for the existence

of each is determined. Global asymptotic stability of one equilibrium is established. In [18], a stability analysis is performed for a simplified model of anaerobic digestion. The model corresponds to continuously stirred bioreactor, with two biomasses (acidogenic and methanogenic microorganisms) and three substrates (simple substrate, acetic acid, and ammonia). The specific growth rate of the methanogenic microorganisms involves inhibition dependence on acetic acid and ammonia. There are four equilibria, some of which involve the existence of one biomass. Their local stability analysis is proved for different cases of the input concentration of simple substrates (s^o) whereas global stability is proved for some cases of low s^o. In [11], a stability analysis is performed for a microalgal pond with nitrification, whose model corresponds to that of a continuously stirred bioreactor with two biomass species (nitrifying biomass and microalgal biomass) and two substrates (ammonium concentration and nitrate concentration). Based on the Lyapunov function method, the global asymptotic stability of the equilibria is proved. There are different equilibrium points, corresponding to the following cases: washout of both biomasses; existence of one biomass; and existence of two biomasses. The conditions for the existence of these equilibrium points are determined, and their local and global stability are determined. In [22] a global stability analysis is performed for a wastewater treatment process whose model corresponds to continuously stirred bioreactor with three substrates (organic nitrogen, NH_4^+-N, and NO_2^-+NO_3^-). The specific reaction rates are Monod type, and the dilution rate is considered constant, whereas the inlet concentration of organic nitrogen is considered time-varying and bounded, so that the system converges to a compact set instead of an equilibrium point. Only normal operation is considered, with no biomass washout. The convergence sets are determined, and global convergence is proved. To this end, dead-zone Lyapunov functions are used.

In cases that the dilution rate (D) is neither fixed nor controlled, the state variables converge to a region instead of an equilibrium point. This case is addressed in [3], where the stability of a simple chemostat model is studied, considering the concentrations of biomass and substrate as state variables, non-monotonic specific growth rate, and random disturbances on the input flow rate. The perturbations on the input flow rate are modeled through bounded random fluctuations. Positive constant lower and upper bounds are considered for the dilution rate. Biomass concentration can exhibit either extinction, weak persistence or strong persistence, depending on the bounds of the dilution rate constraint. The occurrence of these biomass behaviors is proved, and the respective dilution rate range is given. In addition, the convergence regions of substrate and biomass concentrations are determined for the case of biomass persistence. To this end, a comparison of solutions of scalar differential equations, and theory of asymptotically autonomous dynamical systems are used.

In this work, the global stability of a model of continuous bioreactor is studied. The concentrations of biomass and substrate are the state variables, whereas non-monotonic and monotonic functions of substrate concentration are used for the specific growth rate, and the inlet substrate concentration is considered constant. Also, the dilution rate is time varying but bounded, thus leading to the convergence of biomass and substrate concentrations to a compact set instead of an equilibrium point. Based on Lyapunov function theory with dead-zone modification, global stability is studied and proved. Finally, these results are illustrated by numerical simulation of a continuous bioreactor, considering non-monotonic and a monotonic specific growth rates. The main contributions with respect to closely related studies are:

- *Contribution CA*. The convergence regions of the substrate and biomass concentrations are determined as a function of the upper bound of the dilution rate (D), and the global asymptotic convergence to these compact sets is proved, considering the persistent variation of D. In contrast, in

stability studies of open loop continuous bioreactor model based on Lyapunov function, D is commonly considered constant and substrate concentration converges to a point, not a compact set (for instance [9,11,18,19,23]. In addition, the working volume is not assumed constant, which is in contrast to other studies based on the Lyapunov function, for instance [3,11,18,22].

- *Contribution CB*. Several improvements are proposed in the stability analysis, including the definition of a new dead zone Lyapunov function and the properties of its gradient. These improvements allow proving global convergence of substrate and biomass concentrations to their compact sets, while tackling: a) The interwoven and nonlinear nature of the dynamics of biomass and substrate concentrations, b) the non-monotonic nature of the specific growth rate; c) the time-varying nature of the dilution rate. These improvements are a basis for further global stability analysis of bioreactor models exhibiting convergence to a compact set instead of convergence to an equilibrium point. In contrast: i) Challenges a and c are not considered in [22], which is based on dead-zone Lyapunov function theory; ii) other global stability studies based on dead-zone Lyapunov function (for instance [24–27]) are applied to closed-loop systems and are not straightforwardly applicable to the considered bioreactor; iii) global stability studies based on Lyapunov function prove state convergence to compact sets, including the finite-time Lyapunov theory [28–33] and the ultimate bound approach [34–38] but they are not straightforwardly applicable to the considered bioreactor.

The work is organized as follows. The bioreactor model is presented in Section 2. The main results are presented in Section 3. The discussion is presented in Section 4. Numerical simulations are presented in Section 5. The conclusions are drawn in Section 6.

2. Bioreactor model

Consider a continuous flow bioreactor described by model [3,8,39,40]:

$$\frac{dx}{dt} = (\mu - D(t))x \tag{1a}$$

$$\frac{ds}{dt} = (s_{in} - s)D(t) - y_s\mu x \tag{1b}$$

where x and s are the concentrations of biomass and substrate, respectively; μ is the specific growth rate; y_s is the substrate to biomass yield, $y_s\mu x$ is the specific substrate consumption rate; s_{in} is the input substrate concentration; Q_{in} is the input flow rate of medium, Q_{out} is the output flow rate of medium, and v is the volume of the medium in the bioreactor vessel; and $D(t) = Q_{in}/v$ is the dilution rate. If the bioreactor works as an original chemostat, the input and output flow rates are the same ($Q_{in}=Q_{out}$) so that the working volume v is constant [3]. The t argument is hereafter dropped for the sake of simplicity.

The following assumptions are considered:

Assumption 1. The biomass and substrate concentrations feature $x \in (0, \infty)$, $s \in (0, S_{in})$ [33].

Assumption 2. y_s and s_{in} are positive and constant [3,39,40].

Assumption 3. The specific growth rate μ is a continuous function of the substrate concentration (s): it is non-negative, it is either monotonic or non-monotonic, it may involve growth threshold, and it satisfies the following features:

- Non-monotonic case:

$$\begin{cases} \mu \geq 0 \\ \mu \text{ is decreasing for } s \in \left(S_{\mu max}, S_{in}\right) \\ \mu \text{ is increasing for } s \in \left(\underline{s}, S_{\mu max}\right) \text{ and } \mu = 0 \text{ for } s \in [0 \; \underline{s}] \\ or \; \mu \text{ is increasing for } s \in \left(0, S_{\mu max}\right) \end{cases} \quad (2)$$

where $S_{\mu mx} = \underset{s \in (0, \; s_{in})}{arg \; sup} \; \mu$, and $\underline{s}$ is a constant value in the range $(0, S_{\mu mx})$.

- Monotonic case:

$$\begin{cases} \mu \geq 0 \\ \mu \text{ is increasing for } s \in \left(\underline{s}, S_{in}\right) \text{ and } \mu = 0 \text{ for } s \in [0 \; \underline{s}] \\ or \; \mu \text{ is increasing for } s \in (0, S_{in}) \end{cases} \quad (3)$$

where $\underline{s}$ is a constant value in the range $(0, S_{in})$.

Remark 2.1. The features of the non-monotonic growth rate (2) are based on [3,40,41], considering the growth threshold of [42]. Nonmonotone functions describe the case that substrate limits growth at low concentrations, but it is inhibitory at high concentrations [43–45]. As some examples of substrate induced inhibition, *Candida utilis* is inhibited by butanol [46]. *A. succinogenes* is inhibited by sugar [47], *Nitrobacter* is inhibited by nitrite and *Nitrosomas* is inhibited by ammonia [48]. A common nonmonotone function is the Andrews model [3,48,49].

$$\mu_s = \mu_o \frac{s}{k_s + s + \frac{s^2}{k_i}} \quad (4)$$

where k_s, k_i are saturation and inhibition constants, and s is the substrate concentration. The coordinates of the maximum are:

$$\mu_{max} = \mu_o \frac{\sqrt{k_i k_s}}{2k_s + \sqrt{k_i k_s}}, \; S_{\mu mx} = \sqrt{k_i k_s} \quad (5)$$

where μ_{max} is the maximum specific growth rate attainable in presence of inhibition, and $S_{\mu mx}$ is the substrate concentration at maximum specific growth rate. Growth is inhibited and μ_s is decreasing for $s > S_{\mu mx}$ [48].

Remark 2.2. The features of the monotonic growth rate (3) are based on [17,39,41], considering the growth threshold of [42]. A basic example of monotonic growth rate (3) with growth threshold is obtained by using the Monod growth rate function:

$$\mu_s = \begin{cases} \mu_{mx} \frac{s}{k_s + s} - k_o & for \; s > k_s k_o / (\mu_{mx} - k_o) \\ 0 & for \; s \leq k_s k_o / (\mu_{mx} - k_o) \end{cases} \quad (6)$$

where $\mu_{mx} > k_o$, whereas μ_{mx}, k_s, k_o are positive.

Remark 2.3. Growth ceasing for low values of substrate concentration has been verified for some strains. This is represented by using zero reaction rate for substrate concentrations lower than a threshold $\underline{s}$ [42,50].

Remark 2.4. In the case that $s = s_{in}$ for $t = t_o$, Eq (1b) leads to $ds/dt = -y_s \mu x < 0$, what implies $s < s_{to}$ for $t > t_o$, where s_{to} is s at initial time.

3. Analysis of convergence to compact set

In this section, the global stability of model (1) with convergence to a compact set is studied, considering non-monotonic and monotonic growth functions:

i)   The dynamics of transformed states of biomass and substrate concentrations and the summary of the stability analysis procedure is given in subsection 3.1. The dynamics of the transformed states is a necessity for the Lyapunov-based stability analysis.

ii)   The convergence regions of the substrate and biomass concentrations are given in terms of the upper bound of the dilution rate (D), and the global asymptotic convergence to these compact sets is stated in subsection 3.2; the non-monotonic growth function (2) is considered in Theorem 3.1, and the monotonic growth function (3) is considered in Theorem 3.2.

iii) An overview of the proposed improvements of the stability analysis necessary for proving convergence of the substrate and biomass concentrations to their compact sets is given in subsection 3.3, including the proposed dead-zone Lyapunov function and the defined properties of the gradient W.

iv) The relationship of results stated in Theorems 3.1 and 3.2 with equilibrium points is given in subsection 3.4.

3.1. Dynamics of the transformed states and overview of the stability analysis procedure

Consider the bioreactor model (1), subject to assumptions 1 to 3. Let $z = y_s x + s$. Differentiating with respect to time and using the time derivatives (1a), (1b) yields

$$\dot{z} = (s_{in} - z)D$$

Let $\bar{z} = y_s x + s - s_{in}$. Differentiating with respect to time and arranging, yields

$$\frac{d\bar{z}}{dt} = -\bar{z}D \tag{7}$$

The error of substrate concentration is defined as $e = s - s^*$. The constant s^* is:

•   The lowest constant value that satisfies $\mu = D_{max}$ at $s = s^*$ for non-monotonic growth function (2). In this case, two s values satisfy $\mu = D_{max}$, and s^* is the lowest of them.

•   The constant substrate concentration value that satisfies $\mu = D_{max}$ at $s = s^*$ for monotonic growth function (3). In this case, only one s value satisfies $\mu = D_{max}$.

Differentiating e with respect to time, yields $\dot{e} = \dot{s}$. Substituting the time derivative of s (1b) and arranging, yields

$$\dot{e} = -y_s(\mu - D)x + (s_{in} - s - y_s x)D$$

Arranging, yields

$$\dot{e} = -y_s(\mu - D)x - \bar{z}D \tag{8}$$

The overall steps of the procedure used in the proofs of Theorems 3.1 and 3.2 are: definition of the error e as the difference between the substrate concentration and the upper limit of its convergence region; determination of the time derivative de/dt; definition of the new state z, consisting on the weighted addition of the biomass and substrate concentrations; determination of the time derivative

dz/dt; definition of the Lyapunov function for z (V_z) and determination of its time derivative (dV_z/dt); definition of the features of the Lyapunov function for e (V_e) and the features of its gradient (W), using dead-zone modification; determination of the (dV_e/dt) expression in terms of the gradient W; definition of the dead zone W function; determination of the V_e function using the defined W function; determination of the $d(V_e + V_z)/dt$ expression in terms of W; arrangement of the $d(V_z + V_e)/dt$ expression in terms of a non-positive function of W, by applying the properties of the defined dead zone W function and determining the properties of its interaction with the μ, $\bar{z}$ terms; determination of the convergence of the substrate concentration; determination of the convergence of biomass concentration.

This procedure aims at identifying the convergence region of the substrate concentration that leads to non-positive nature of the $d(V_e + V_z)/dt$ expression, what in turn allows to prove the convergence. The dead-zone modification is used in the Lyapunov function V_e to facilitate the study of convergence to a compact set instead of an equilibrium point. Dead-zone Lyapunov functions have been mainly used for robust control design: recent studies are presented in [24–27] whereas early studies are presented in [51–53]. In addition, an application to open loop systems is presented in [22].

3.2. Convergence of the substrate and biomass concentrations

Theorem 3.1. Consider the bioreactor model (1) subject to assumptions 1 to 3, with the non-monotonic growth function μ satisfying conditions (2), and the dilution rate D is time-varying and subject to saturation:

$$D \in [0, \quad D_{max}] \tag{9}$$

$$0 < D_{max} < \mu_{sin}$$

$$D_{max} < \sup_{s \in (0, \quad s_{in})} \mu \tag{10}$$

where μ_{sin} is the μ value at $s = s_{in}$. Then:

    i)   the substrate concentration s converges asymptotically to $\Omega_s = \{s: 0 < s \leq s^*\}$ where s^* is the lowest constant value that satisfies $\mu = D_{max}$ at $s = s^*$;

    ii)   the biomass concentration (x) converges asymptotically to $\Omega_x = \left\{x: \frac{1}{y_s}(s_{in} - s^*) \leq x < \frac{1}{y_s}s_{in}\right\}$.

Proof. Expression (8) involves both s and $\bar{z}$ with nonlinear dependence on s, and time varying dilution rate (D). Then, choosing a Lyapunov function that allows proving the convergence of e is overly complex. To this end, the Lyapunov function V_e is defined in terms of its gradient W, and the properties of V_e, W are also defined at this point, but the V_e, W expressions are defined at the last part of the stability analysis. The main features of V_e are:

$$V_e = 0 \quad for \ e \leq 0$$

$$V_e > 0 \quad for \ e > 0 \tag{11}$$

V_e *is continuous with respect to* e, and it is bounded for bounded e

V_e *is non* $-$ *decreasing with respect to* $e, for \ e > 0$

The time derivative of V_e can be expressed as

$$\frac{dV_e}{dt} = W\frac{de}{dt} \tag{12}$$

Where the gradient of V_e is:

$$W = \frac{dV_e}{de} \tag{13}$$

The properties of W in terms of e are:

$$W = 0 \ \ for \ \ e \leq 0$$

$$W > 0 \ \ for \ \ e > 0 \tag{14}$$

$$W \ \ is \ \ continuous \ \ with \ \ respect \ \ to \ \ e$$

$$W \ \ is \ \ non-decreasing \ \ with \ \ respect \ \ to \ \ e, for \ \ e > 0$$

The V_e function can be determined from the integrated form of Eq (13):

$$V_e = \int_0^e W de \tag{15}$$

The resulting V_e function fulfills properties (11). Combining Eq (12) with the de/dt expression (8), yields

$$\frac{dV_e}{dt} = -y_s W(\mu - D)x - W\bar{z}D$$

Which can be rewritten as

$$\frac{dV_e}{dt} = -\varepsilon_a y_s W(\mu - D)x - \varepsilon_b y_s W(\mu - D)x - W\bar{z}D \tag{16}$$

Where ε_a, ε_b are positive constants fulfilling

$$\varepsilon_a + \varepsilon_b = 1; \ \ \varepsilon_a \in (0, \ 1); \ \ \varepsilon_b \in (0, \ 1)$$

From the definition of s^*, the dependence of μ on s (2) and the limitation of D_{max} (10) it follows that

$$\mu > D_{max} \ \ for \ \ s > s^* \ \ and \ \ \mu = D_{max} \ \ for \ \ s = s^* \tag{17}$$

Hence, $\mu - D_{max} > 0 \ \ for \ \ e > 0$. Considering the limitation of D (9), we get

$$\mu - D \geq \mu - D_{max} > 0 \ \ \ for \ \ e > 0 \tag{18}$$

Combining with the W properties (14), we have $W(\mu - D) = 0$ for $s \leq s^*$ and $W(\mu - D) > 0$ for $s > s^*$. Therefore,

$$-\varepsilon_b y_s W(\mu - D)x \leq -\varepsilon_b y_s W(\mu - D_{max})x$$

Hence, a preliminary W function is chosen to be

$$W_p = \begin{cases} \mu - D_{max} & for \quad s \geq s^* \\ 0 & for \quad s < s^* \end{cases}$$

Which does not satisfy the last of W properties (14), because of the non-monotonic nature of μ. From Eq (17) and the fact that $\mu = \mu_{sin}$ for $s = s_{in}$, it follows that μ is higher than the line that connects the points (s^*, D_{max}) and (s_{in}, μ_{sin}):

$$\mu > D_{max} + \left(\frac{\mu_{sin} - D_{max}}{s_{in} - s^*}\right)(s - s^*) \quad for \quad s \in (s^*, s_{in})$$

$$\mu \geq D_{max} + \left(\frac{\mu_{sin} - D_{max}}{s_{in} - s^*}\right)(s - s^*) \quad for \quad s \in [s^*, s_{in}] \tag{19}$$

Therefore, the W function is chosen to be

$$W = \begin{cases} \left(\frac{\mu_{sin} - D_{max}}{s_{in} - s^*}\right)e & for \quad e \geq 0 \\ 0 & for \quad e < 0 \end{cases} \tag{20}$$

Which satisfies W properties (14). In addition, the resulting Lyapunov function V_e can be obtained by using Eqs (15) and (20):

$$V_e = \begin{cases} \left(\frac{\mu_{sin} - D_{max}}{s_{in} - s^*}\right)\frac{e^2}{2} & for \quad e \geq 0 \\ 0 & for \quad e < 0 \end{cases} \tag{21}$$

Equations (14), (18), (19) and (20) imply

$$W(\mu - D) \geq W^2 \geq 0 \tag{22}$$

The proof is given in Appendix A1. From this property and the positiveness of x stated in assumption 1, it follows that

$$-\varepsilon_b y_s W(\mu - D)x \leq -\varepsilon_b y_s \, x_{min} W^2$$

$$x_{min} = \inf_t x$$

Substituting in Eq (16), yields

$$\frac{dV_e}{dt} \leq -\varepsilon_a y_s W^2 x - \varepsilon_b y_s x_{min} W^2 - W\bar{z}D \tag{23}$$

In view of the effect of $\bar{z}$, we consider the Lyapunov function for it:

$$V_z = \frac{1}{2}k_z \bar{z}^2 \tag{24}$$

which exhibits the following properties:

$$V_z = 0 \quad for \quad \bar{z} = 0$$

$$V_z > 0 \quad for \quad \bar{z} \neq 0 \tag{25}$$

V_z *is continuous with respect to* $\bar{z}$, and it is bounded for bounded $\bar{z}$

V_z *is increasing with respect to* $|\bar{z}|$

Differentiating V_z with respect to time, using Eq (7), yields

$$\dot{V}_z = -k_z D\bar{z}^2$$

Combining with Eq (23), yields

$$\frac{dV_e}{dt} + \frac{dV_z}{dt} \leq -\varepsilon_a y_s W^2 x - \varepsilon_b y_s x_{min} W^2 - W\bar{z}D - k_z D\bar{z}^2 \tag{26}$$

Where

$$-\varepsilon_b y_s x_{min} W^2 - W\bar{z}D - k_z D\bar{z}^2 \leq 0$$

$$for \quad k_z = \frac{D_{max}}{4\varepsilon_b y_s x_{min}}$$

Substituting into Eq (26), yields

$$\frac{dV_e}{dt} + \frac{dV_z}{dt} \leq -\varepsilon_a y_s W^2 x$$

Considering assumption 1, yields

$$\frac{dV_e}{dt} + \frac{dV_z}{dt} \leq -\varepsilon_a y_s W^2 x_{min} \leq 0 \tag{27}$$

Arranging and integrating, yields

$$V_e + V_z + \varepsilon_a y_s x_{min} \int_0^t W^2 dt \leq V_{eto} + V_{zto} \tag{28}$$

where V_{eto} is V_e at initial time, whereas V_{zto} is V_z at initial time. From (28) it follows that $V_e \in \mathcal{L}_\infty$, $V_z \in \mathcal{L}_\infty$, $W_a^2 \in \mathcal{L}_1$. Applying the Barbalat's lemma [54], yields

$$\lim_{t\to\infty} W^2 = 0$$

And consequently,

$$\lim_{t\to\infty} W = 0$$

Accounting for the W properties (14) and the substrate positiveness constraint stated in assumption 1, we deduce that s converges asymptotically to $\Omega_s = \{s : 0 < s \leq s^*\}$.

From Eq (7) it follows that $\bar{z} = y_s x + s - s_{in}$ converges exponentially to zero. This result and the asymptotic convergence of s to Ω_s imply that x converges asymptotically to

$$\Omega_x = \left\{ x : \frac{1}{y_s}(s_{in} - s^*) \leq x < \frac{1}{y_s} s_{in} \right\}$$

This completes the proof.

Remark 3.1. The value $\mu = D_{max}$ holds true for two values of substrate concentration (s), for non-monotonic specific growth rate μ, and s^* is the lowest of them.

Remark 3.2. The fulfillment of the W properties (14) leads to the fulfillment of the V_e properties (11). In addition, V_z (24) exhibits the properties (25).

Remark 3.3. In Theorem 3.1, the conditions $0 < D_{max} < \mu_{sin}$, $D_{max} < \sup_{s \in (0, \ s_{in})} \mu$ imply

$$D_{max} < min\left\{ \mu_{sin}, \sup_{s \in (0, \ s_{in})} \mu \right\} = \mu_{sin}$$

because $\mu_{sin} \leq \underset{s \in (0, \ s_{in})}{sup} \mu.$

Remark 3.4. Condition $0 < D_{max} < \mu_{sin}$ implies that only one s value (s^*) satisfies both $\mu|_{s=s^*} = D_{max}$ and $s < s_{in}$.

Theorem 3.2. Consider the bioreactor model (1) subject to assumptions 1 to 3, with the monotonic growth function μ, satisfying conditions (3), and the dilution rate D is time varying and subject to saturation:

$$D \ \in [0, D_{max}] \tag{29}$$

$$0 < D_{max} < \mu_{sin} \tag{30}$$

Where μ_{sin} is the μ value at $s = s_{in}$. Then:

i) the substrate concentration converges asymptotically to $\Omega_s = \{s : 0 < s \leq s^*\}$ where s^* is a constant substrate concentration value that satisfies $\mu = D_{max}$ at $s = s^*$;

ii) the biomass concentration (x) converges asymptotically to $\Omega_x = \left\{x : \frac{1}{y_s}(s_{in} - s^*) \leq x < \frac{1}{y_s}s_{in}\right\}.$

Proof. The transformed states e, $\bar{z}$ are defined as

$$e = s - s^*, \ \bar{z} = y_s x + s - s_{in}$$

The time derivative of e is given by Eq (8), whereas the time derivative of $\bar{z}$ is given by Eq (7). Consider the Lyapunov function

$$V = V_e + V_z \tag{31}$$

Where

$$V_z = \frac{1}{2}k_z \bar{z}^2, \ V_e = \int_0^e W de$$

and the gradient function W satisfies the properties in terms of e:

$$W = 0 \quad for \ e \ \leq 0$$

$$W \ > 0 \quad for \ \ e > 0 \tag{32}$$

$$W \ is \ continuous \ with \ respect \ to \ e$$

$$W \ is \ non-decreasing \ with \ respect \ to \ e, for \ e > 0$$

Differentiating V (31) with respect to time, using the time derivatives of e and $\bar{z}$ given by Eqs (8), (7), yields

$$\frac{dV_e}{dt} + \frac{dV_z}{dt} \leq -\varepsilon_a y_s W(\mu - D)x \tag{33}$$

From the definition of s^*, the dependence of μ on s (3), and the limitation of D_{max} (30), it follows that $\mu > D_{max}$ for $s > s^*$ and $\mu = D_{max}$ for $s = s^*$. Hence, $\mu - D_{max} > 0$ for $e > 0$ and $\mu - D_{max} = 0$ for $e = 0$. Considering the limitation of D (29), we have

$$\mu - D \geq \mu - D_{max} > 0 \quad \text{for} \ \ e > 0 \tag{34}$$

Then, considering the W properties (32), the exact W function is chosen as

$$W = \begin{cases} \mu - D_{max} & for \quad e \geq 0 \\ 0 & for \quad e < 0 \end{cases} \tag{35}$$

Which satisfies properties (32). In addition, the resulting Lyapunov function V_e can be obtained from Eq (15):

$$V_e = \begin{cases} \int_0^e (\mu_e - D_{max}) \, de & for \quad e \geq 0 \\ 0 & for \quad e < 0 \end{cases} \tag{36}$$

Where μ_e is the μ function with the state transformation $s = e + s^*$. From the W definition (35) and properties (34), (32) it follows that

$$\mu - D \geq W > 0 \quad for \ \ e > 0$$

Combining with the second subequation of (32), yields

$$W(\mu - D) \geq W^2 > 0 \quad for \ \ e > 0 \tag{37}$$

From the first subequation of (32), it follows that

$$W(\mu - D) = 0 = W^2 \quad for \ \ e \leq 0$$

Combining with (37), yields

$$W(\mu - D) \geq W^2 \geq 0$$

Using this result in Eq (33), yields

$$\frac{dV_e}{dt} + \frac{dV_z}{dt} \leq -\varepsilon_a y_s W^2 x \leq 0$$

Considering assumption 1, yields

$$\frac{dV_e}{dt} + \frac{dV_z}{dt} \leq -\varepsilon_a y_s W^2 x_{min} \leq 0$$

Arranging and integrating, yields

$$V_e + V_z + \varepsilon_a y_s x_{min} \int_0^t W^2 dt \leq V_{eto} + V_{zto}$$

Hence, $V_e \in \mathcal{L}_\infty, V_z \in \mathcal{L}_\infty, W^2 \in \mathcal{L}_1$. Applying the Barbalat's lemma [54], yields

$$\lim_{t \to \infty} W^2 = 0$$

And consequently,

$$\lim_{t \to \infty} W = 0$$

Accounting for the W definition (35) and the substrate positiveness constraint stated in assumption 1, we deduce that s converges asymptotically to $\Omega_s = \{s: 0 < s \leq s^*\}$.

From Eq (7) it follows that $\bar{z} = y_s x + s - s_{in}$ converges exponentially to zero. This result and the asymptotic convergence of s to Ω_s imply that x converges asymptotically to

$$\Omega_x = \left\{x: \frac{1}{y_s}(s_{in} - s^*) \leq x < \frac{1}{y_s}s_{in}\right\}$$

This completes the proof.

Remark 3.5. Theorem 3.1 considers nonmonotonic growth rate function μ whereas Theorem 3.2 considers monotonic growth rate function.

Remark 3.6. Any time-varying D behavior satisfying $D \in [0, \ D_{max}]$, $0 < D_{max} < \mu_{sin}$ is allowed in Theorems 3.1 and 3.2, including the sinusoidal, random type or a combination of them. Also, constant D behavior is allowed.

Remark 3.7. For the nonmonotonic case, the geometric properties of V_e stated in Eq (11) arise as a consequence of the properties of W stated in Eq (14). Indeed, properties (11) are straightforwardly verified for the Lyapunov function (21). For the monotonic case, the geometric properties of V_e arise as a consequence of the properties of W stated in Eq (32).

3.3. Summary of the proposed improvements of the stability analysis and dead zone Lyapunov function

Proposed improvements of the stability analysis. The improvements proposed in the stability analysis are detailed in the proofs of Theorems 3.1 and 3.2, most of them related to the proposed dead zone Lyapunov function for the tracking error $e = s - s^*$, V_e, and its gradient W. These improvements can be summarized as follows:

- Before defining V_e, the dV_e/dt equation is expressed in terms of the gradient W (see Eqs (12) and (16)) and the properties of W relevant for proving convergence of the tracking error e are defined using dead zone modification, see Eq (14).

- Then, the Lyapunov function V_e is expressed as an integral in terms of its gradient W, see Eq (15).

- A particular dead zone W function is proposed, see Eqs (20) and (36), fulfilling the stated W properties. As a result, a new expression is obtained for V_e, with dead zone modification, see Eqs (21) and (36).

- The $d(V_z + V_e)/dt$ expression is arranged in terms of a non-positive function of W, by applying the properties of the W stated in Eq (14) and determining the properties of the interaction of W with the $\mu, \ \bar{z}$ terms, see Eq (22) and subsequent equations.

Proposed dead zone Lyapunov function and its gradient. The overall Lyapunov function is

$$V = V_z + V_e, \ V_z = \frac{1}{2}k_z\bar{z}^2$$

Where $k_z = D_{max}/(4\varepsilon_b y_s x_{min})$, $\bar{z} = y_s x + s - s_{in}$, and V_e is function of the error $e = s - s^*$, and it is defined in terms of its gradient:

$$V_e = \int_0^e W de \tag{38}$$

The properties of W in terms of the error $e = s - s^*$ are:

$$W = 0 \quad for \quad e \leq 0$$

$$W > 0 \quad for \quad e > 0 \tag{39}$$

$$W \ is \ continuous \ with \ respect \ to \ e$$

$$W \ is \ non-decreasing \ with \ respect \ to \ e, for \ e > 0$$

A particular W function that satisfies these properties, for the case of non monotonic specific growth rate (2), is:

$$W = \begin{cases} \left(\frac{\mu_{sin} - D_{max}}{s_{in} - s^*}\right) e & for \quad e \geq 0 \\ 0 & for \quad e < 0 \end{cases} \tag{40}$$

For which the Lyapunov function V_e is found by using Eq (38):

$$V_e = \begin{cases} \left(\frac{\mu_{sin} - D_{max}}{s_{in} - s^*}\right) \frac{e^2}{2} & for \quad e \geq 0 \\ 0 & for \quad e < 0 \end{cases} \tag{41}$$

A particular W function that satisfies properties (39), for the case of monotonic specific growth rate (3), is:

$$W = \begin{cases} \mu - D_{max} & for \quad e \geq 0 \\ 0 & for \quad e < 0 \end{cases} \tag{42}$$

For which the Lyapunov function V_e is:

$$V_e = \begin{cases} \int_0^e (\mu_e - D_{max}) \, de & for \quad e \geq 0 \\ 0 & for \quad e < 0 \end{cases} \tag{43}$$

Where μ_e is the μ function with the state transformation $s = e + s^*$. Both W functions (40) and (42) fulfill

$$W(\mu - D) \geq W^2 \geq 0$$

In the case of Monod growth function with growth threshold (6), the Lyapunov expression V_e (43) gives:

$$V_e = \begin{cases} \mu_{mx}\left[e - k_s ln\left(\frac{k_s + e + s^*}{k_s + s^*}\right)\right] - (k_o + D_{max})e & for \quad e \geq 0 \\ 0 & for \quad e < 0 \end{cases} \tag{44}$$

Remark 3.8. The results stated in Theorems 3.1 and 3.2 and their proofs do not allow stating the input to state stability (ISS) of system (1), in the context of the ISS notion stated in [55]. One way to prove that a system is ISS is by proving that the existence of an ISS Lyapunov function. An ISS Lyapunov function satisfies

$$\alpha_1(|y|) \leq V(y) \leq \alpha_2(|y|) \tag{45}$$

$$\frac{dV}{dt} \leq -\alpha_2(|y|) + \alpha_4(\|u\|)$$

Where y is the state vector, u is the input; $\alpha_1, \alpha_2, \ \alpha_3, \ \alpha_4$ are $\mathcal{K}_\infty$ functions, according to

[55]. In Eqs (26) and (27):

i)   The term $-\varepsilon_a y_s W^2 x_{min}$ is not $\mathcal{K}_\infty$, because W^2 is not strictly increasing, according to Eq (14). Indeed, it is not increasing for $e \leq 0$.

ii)   The Lyapunov function $V = V_e + V_z$ does not satisfy condition (45) because V_e is not strictly increasing.

Then, ISS property cannot be concluded. However, Theorems 3.1 and 3.2 and their proofs allow stating the boundedness for bounded input D. Equation (28) implies that e, z are bounded, and consequently x, s are bounded, provided bounded D.

3.4. Relationship with equilibrium points

Notice that the limits of the convergence regions of x, s stated in Theorem 3.1 are related to one of the equilibrium points of model (1). Model (1) with nonmonotonic growth rate (4) and constant dilution rate D exhibits the equilibrium points:

$$E_1: \begin{cases} x^{eq} = \dfrac{1}{y_s}\left\{ s_{in} + \dfrac{(D-\mu_o)+\sqrt{(D-\mu_o)^2-4(k_s/k_i)D^2}}{2D/k_i} \right\} \\[3mm] s^{eq} = \dfrac{-(D-\mu_o)-\sqrt{(D-\mu_o)^2-4\left(\frac{k_s}{k_i}\right)D^2}}{2D/k_i} \\[3mm] D < \mu_o \dfrac{\sqrt{k_i k_s}}{2k_s+\sqrt{k_i k_s}} \end{cases} \tag{46}$$

$$E_2: \begin{cases} x^{eq} = \dfrac{1}{y_s}\left\{ s_{in} + \dfrac{(D-\mu_o)-\sqrt{(D-\mu_o)^2-4(k_s/k_i)D^2}}{2D/k_i} \right\} \\[3mm] s^{eq} = \dfrac{-(D-\mu_o)+\sqrt{(D-\mu_o)^2-4\left(\frac{k_s}{k_i}\right)D^2}}{2D/k_i} \\[3mm] D < \mu_o \dfrac{\sqrt{k_i k_s}}{2k_s+\sqrt{k_i k_s}} \end{cases} \tag{47}$$

$$E_3: \begin{cases} x^{eq} = 0 \\ s^{eq} = s_{in} \end{cases} \tag{48}$$

The upper limit of the convergence region of s, that is, $s^* = \dfrac{-(D_{max}-\mu_o)-\sqrt{(D_{max}-\mu_o)^2-4\left(\frac{k_s}{k_i}\right)D_{max}^2}}{2D_{max}/k_i}$,

obtained from condition $\mu = D_{max}$ at $s = s^*$, that is, $\mu = \mu_o \dfrac{s}{k_s+s+\frac{s^2}{k_i}}\bigg|_{s=s^*} = D_{max}$ corresponds to

equilibrium point E_1 with constant $D = D_{max}$. The limits of the convergence region of x, that is

$\dfrac{1}{y_s}(s_{in} - s^*) = \dfrac{1}{y_s}\left\{ s_{in} + \dfrac{(D_{max}-\mu_o)+\sqrt{(D_{max}-\mu_o)^2-4(k_s/k_i)D_{max}^2}}{2D_{max}/k_i} \right\}$ and $\dfrac{1}{y_s}s_{in}$,   correspond to the

equilibrium point E_1, with constant $D = D_{max}$ and constant $D = 0$, respectively.

Also, notice that the limits of the convergence regions of x, s stated in Theorem 3.2 are related to one of the equilibrium points of model (1). Model (1) with monotonic growth rate $\mu = \mu_{mx}\dfrac{s}{k_s+s}$ and constant dilution rate D exhibits the equilibrium points

$$E_1: \begin{cases} x^{eq} = \dfrac{1}{y_s}\left(s_{in} - \dfrac{k_s D}{\mu_{mx} - D}\right) \\ s^{eq} = \dfrac{k_s D}{\mu_{mx} - D} \\ D < \mu_{mx} \end{cases}$$

$$E_2: \begin{cases} x^{eq} = 0 \\ s^{eq} = s_{in} \end{cases}$$

The upper limit of the convergence region of s, obtained from condition $\mu = D_{max}$ at $s = s^*$, is $s^* = \dfrac{k_s D_{max}}{\mu_{mx} - D_{max}}$, and it corresponds to equilibrium point E_1 with constant $D = D_{max} < \mu_{mx}$. The limits of the convergence region of x, that is, $\dfrac{1}{y_s}(s_{in} - s^*) = \dfrac{1}{y_s}\left(s_{in} - \dfrac{k_s D_{max}}{\mu_{mx} - D_{max}}\right)$ and $\dfrac{1}{y_s}s_{in}$, correspond to the equilibrium point E_1 with constant $D = D_{max}$ and constant $D = 0$, respectively. In summary, the limits of the convergence regions of x, s stated in Theorems 3.1 and 3.2 correspond to the equilibrium point E_1 with constant $D = D_{max}$ and constant $D = 0$.

Remark 3.9. Consider the case that model (1) with constant dilution rate

$$D = \sup_{s < s_{in}} \mu$$

and Haldane kinetics (4), so that

$$D = \mu_{max} = \mu_o \frac{\sqrt{k_i k_s}}{2k_s + \sqrt{k_i k_s}}.$$

This D value does not fulfill conditions (9) and (10), so that neither Theorem 3.1 nor 3.2 apply, and the constant nature of D implies that the states converge to equilibrium point, not to compact set, so that dead-zone modification of the Lyapunov function is not necessary. In this case, the D value implies that there is only two equilibrium points, and Eqs (46)–(48) lead to:

$$E_1: \begin{cases} x^{eq} = \dfrac{1}{y_s}\left\{s_{in} + \dfrac{(D - \mu_o)}{2D/k_i}\right\} \\ s^{eq} = \dfrac{-(D - \mu_o)}{2D/k_i} \\ D = \mu_o \dfrac{\sqrt{k_i k_s}}{2k_s + \sqrt{k_i k_s}} \end{cases} \tag{49}$$

$$E_2: \begin{cases} x^{eq} = 0 \\ s^{eq} = s_{in} \end{cases} \tag{50}$$

In addition, equilibrium E_1 is a pitchfork bifurcation point with respect to parameter D, so that its local stability cannot be stated through eigenvalues, and other stability tools for bifurcations are necessary, see for instance [56,57].

4. Discussion

4.1. General discussion of results

The stability analysis summarized in Theorems 3.1 and 3.2 determines global convergence of

biomass and substrate concentrations from the model (1) towards a compact set. Assumptions 1 to 3 are considered, the specific growth rate function is assumed to be a nonlinear function of substrate concentration, either non-monotonic (2) or monotonic (3), with constant inflow substrate concentration. The dilution rate (D) is varying within the compact set $\Omega_D = \{D: 0 \leq D \leq D_{max}\}$, implying that the states x, s converge to the compact sets Ω_s, Ω_x instead of an equilibrium point. Common global stability of open loop continuous bioreactor model based on the Lyapunov function (for instance [9,11,18,19,23]) cannot be used for this case, because they consider constant dilution rate D and convergence of substrate and biomass concentrations towards a point, not a compact set.

To this end, methods that consider state convergence to compact set include the comparison of solutions of scalar differential equations and theory of asymptotically autonomous dynamical systems [3]; dead zone Lyapunov functions [24–27], and ultimate bound approach [34–38]. The dead zone Lyapunov method is commonly used for control design, so that its application for bioreactor systems as the model (1) is hampered by the nonlinear μ term and the complex nonlinear connection between the dynamics of x, s. The application of the ultimate bound approach is also hampered by these facts.

Results related to Contribution CA. Theorems 3.1 and 3.2 indicate the global convergence of substrate concentration s to the compact set $\Omega_s = \{s: 0 < s \leq s^*\}$ and the global convergence of biomass concentration x to the compact set $\Omega_x = \{x: (1/y_s)(s_{in} - s^*) \leq x < (1/y_s)s_{in}\}$, and also provide a persistent condition $(0 < D_{max} < \mu_{sin})$ that leads to biomass persistence (avoidance of washout) for the case of nonmonotonic growth rate function, where s^* is the solution of $\mu = D_{max}$ for $s = s^*$. The limit value s^* is a function of D_{max}, so that the widths of Ω_s, Ω_x depend on the width of Ω_D.

Results related to Contribution CB. The stability proofs of Theorems 3.1 and 3.2 in subsection 3.2 use the Lyapunov function method with dead zone modification. However, the stability analysis is significantly improved, and a new dead-zone Lyapunov function (V_e) is proposed, in order to prove global convergence of substrate and biomass concentrations to their compact sets Ω_s, Ω_x while tackling the non-linear nature of the specific growth rate μ, the interwined dynamics of the concentrations of substrate and biomass, and the variation of the dilution rate (D) within the compact set Ω_D. Indeed, the properties of V_e and of its gradient W are defined and used for the stability analysis but the exact W and V_e expressions are provided at the last part of the stability analysis. Some remarkable features are:

- The properties of W in Eq (39) indicate that W is continuous, piecewise, dependent on $e = s - s^*$, increasing for $e > 0$ and involving a vanishing region for $e \leq 0$.
- In the case of non-monotonic μ (2), μ is only increasing for a certain range of $e > 0$, so that it does not lead to increasing W. Thus, W is defined as a piecewise linear function of e, including no section of the μ curve, see Eq (40).
- In the case of monotonic μ (3), μ leads to increasing W function. Thus, the W definition includes a section of the μ curve, see Eq (42).
- The equation of V_e as an integral in terms of W (38) allows obtaining the V_e functions (41) and (43).

In addition, the improved stability analysis (Theorems 3.1 and 3.2 and their proofs) is useful as the procedure for further global stability analysis of bioreactor models exhibiting convergence to a compact set instead of convergence to an equilibrium point, allowing the determination of:

- R1: range of initial values of the state variables and parameter values leading to global convergence to the non-washout convergence set (washout avoidance) in the case in the case of nonmonotonic growth rate function.

- R2: upper bound of the transient values of the state variables as a function of their initial values and model parameters
- R3: exponential, asymptotic, monotonic or nonmonotonic character of the global convergence of the state variables to the compact set

In agreement with R1, the global stability of continuous bioreactors through Lyapunov function allows checkinh domains of attraction of normal operation equilibrium point, under a constant dilution rate [8,18,58].

From the analysis of the relationship between the results stated in Theorems 3.1 and 3.2 with the equilibrium points (in subsection 3.4) it would seem that local stability (equilibrium points and eigenvalues) is enough to study the convergence of the state variables to compact sets. However, local stability does not allow us to obtain results R1, R2 and R3, because it is limited to a close neighborhood of the equilibrium point, and it disregards the transient behavior in regions far from the equilibrium point, as can be deduced from [12,56].

4.2. Future work

An important application field of the stability analysis based on the Lyapunov function presented in Theorems 3.1 and 3.2 and their proofs, is the anaerobic digestion process [18]. Anaerobic digestion is useful for wastewater treatment with biogas production. It involves a complex process with hydrolysis, acidogenesis, acetogenesis and methanogenesis steps. It is prone to biomass washout, which consists of microorganism extinction, it occurs for overlarge values of dilution rate and is related to high substrate concentration [8,12,59]. The stability of equilibrium points related to normal operation point and washout has been studied through equilibrium points, diagrams of equilibrium versus dilution rate, bifurcation diagrams with dilution rate and input substrate concentration as bifurcation parameters [12,56,59]. In contrast, global stability based on the Lyapunov function gives as result the conditions and the state space region that implies global stability of the normal operation equilibrium point, considering constant dilution rate [18,58].

Also, the developed stability analysis can be extended to more complex bioreactor models, and modifications of the model (1), including:

- Model of anaerobic upflow fixed-bed digester with partial biomass attachment on support:

$$\frac{dx}{dt} = (\mu - \alpha D)x; \quad \frac{ds}{dt} = (s_{in} - s)D - y_s \mu x$$

where α is a positive constant that represents the model heterogeneity [7,49].

- Model with maintenance term mx:

$$\frac{dx}{dt} = (\mu - D)x; \quad \frac{ds}{dt} = (s_{in} - s)D - (y_s \mu + m)x$$

where m is a postive constant [42].

- Model with several biomass species:

$$\frac{dx_i}{dt} = (\mu_i - D)x_i; \quad \frac{ds}{dt} = (s_{in} - s)D - \sum_{i=1}^{n} y_i \mu_i x_i$$

where x_i is the mass density of species i [60].

These models, combined with either time varying dilution rate (D) or time varying inflow

substrate concentration (s_{in}) leads to different convergence sets for the states x, s. In the case of varying s_{in}, the model for $\bar{z} = y_s x + s - s_{in}$ is modified. The limits of the convergence regions depend on the limits of D, s_{in}.

Some biological models exhibit limit cycles under constant parameters (see [61,62]). It has been suggested that their oscillations are a consequence of competitive interaction and low nutrient supply [63,64]. Simple models with two microbial populations and Monod uptake terms are capable of describing the states of the system with stable oscillations [64]. As an example, in nitrification at the soil with contaminant ammonium plume, bacterial populations exhibit boom and boost dynamics [62]. In these cases, the Lyapunov function is a possible tool for examining the global convergence of the states towards the limit cycle, but other tools are also necessary for proving the existence and stability of the limit cycles (see [65–67]). Indeed, some biological systems are described in predator-prey type models, whereas these models may be taken to polar coordinates so that the differential equation of the radial coordinate indicates that the radius is stable, and a Lyapunov function can be defined in terms of its gradient, see [51,68]. In this case, the dead zone Lyapunov function can provide a more complete stability result.

5. Numerical simulation

In this section, the convergence results stated in theorems 3.1 and 3.2 are illustrated through simulation, by showing the convergence regions of biomass and substrate concentrations (x, s) and the asymptotic convergence of their trajectories towards to convergence regions. Bioreactor model (1) subject to assumptions 1 to 3 is considered, Theorem 3.1 is illustrated in the first simulation example, using a Haldane growth rate function, whereas theorem 3.2 is illustrated in the second simulation example, using a Monod growth rate function.

First simulation example. The simulation conditions correspond to chemostat with bacterial species and Haldane growth rate function (4):

$$\mu_s = \mu_o \frac{s}{k_s + s + \frac{s^2}{k_i}} \tag{51}$$

The parameter values are given in Table 1.

Table 1. Parameter values used in the simulations.

	Specific growth rate	Model parameters	Values of the main points of the specific growth rate function
First simulation example	Non-monotonic, Eq (51)	$\mu_o = 7$ $k_s = 7$ $k_i = 7$ $s_{in} = 16.7$ $D_{max} = 1.65$	$s_{\mu mx} = 7$ $\mu_{max} = 2.333$ $s^* = 2.4161$ $\mu_{sin} = 1.8397$
Second simulation example	Monotonic, Eq (52)	$\mu_{mx} = 0.9972$ h^{-1} $k_s = 681.69$ g/L $k_o = 0.0548$ h^{-1} $s_{in} = 100$ g/L $D_{max} = 0.0582$ h^{-1}	$\mu_{sin} = 0.0728$ h^{-1} $s^* = 87.13$ g/L

For the growth rate function (51), the coordinates of the maximum are given by Eq (5). The D_{max} value satisfies condition (10), and s^* is the lowest solution of $\mu = D_{max}$:
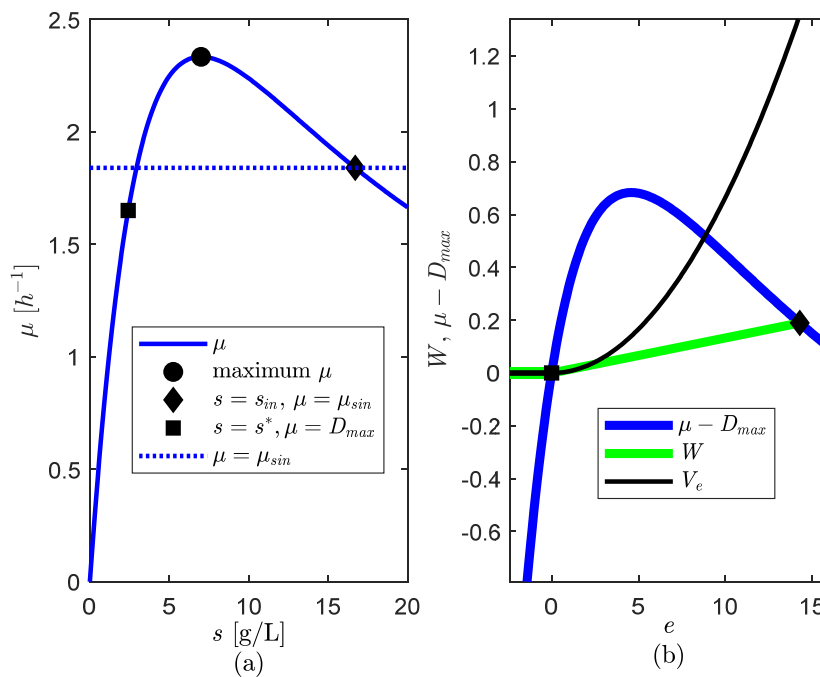
$$\mu_o \left. \frac{s}{k_s + s + \dfrac{s^2}{k_i}} \right|_{s=s^*} = D_{max}$$

what leads to

$$\frac{D_{max}}{k_i}(s^*)^2 + (D_{max} - \mu_o)s^* + D_{max}k_s = 0$$

$$s^* = \frac{-(D_{max} - \mu_o) - \sqrt{(D_{max} - \mu_o)^2 - 4\left(\dfrac{k_s}{k_i}\right)D_{max}^2}}{2D_{max}/k_i}$$

An example of D_{max}, s^* values is given in Table 1. The growth function (51), its main points, the gradient W (40) and Lyapunov function V_e (41) are illustrated in Figure 1.
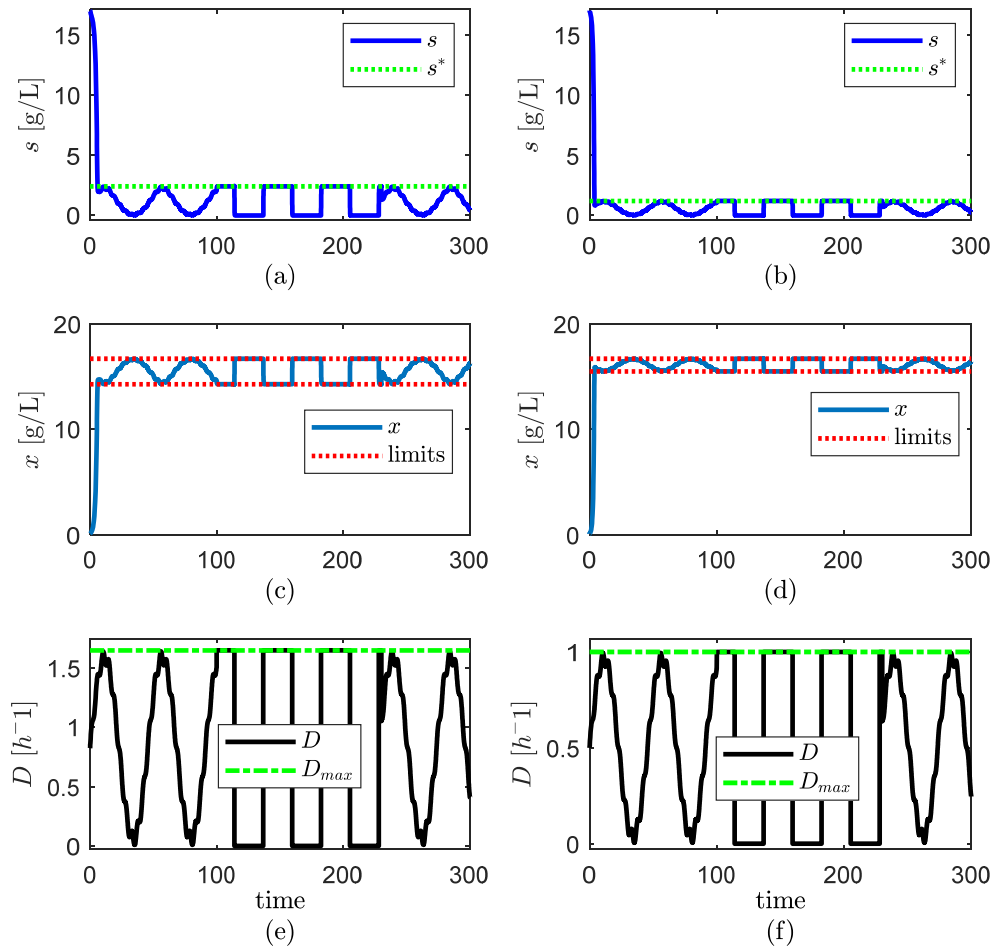

Figure 1. Non monotonic growth rate function and its gradient: (a) non-monotonic function (51); (b) function $\mu - D_{max}$, gradient W and Lyapunov function V_e.

The time varying dilution rate is:

$$D = \begin{cases} 0.5D_{max} + 0.5D_{max}sign\left(\sin\left(\dfrac{2\pi}{\tau_{d1}}t\right)\right) & for \ t \ \in \Omega_{t1} \\ 0.5D_{max} + a_1 0.5D_{max} \sin\left(\dfrac{2\pi}{\tau_{d1}}t\right) + (1 - a_1)0.5D_{max} \sin\left(\dfrac{2\pi}{\tau_{d2}}t\right) & otherwise \end{cases}$$

where $a_1 = 0.93, \tau_{d1} = 45$ $\tau_{d2} = 45/10$ and $\Omega_{t1} = [100, \ 230]$ for $D_{max} = 1.65$ and for $D_{max} = 1$.

Figure 2. Simulation results for first simulation example. Subfigures (a), (c), (e) show the trajectories of the substrate and biomass concentrations and dilution rate signal for $D_{max} = 1.65$. Subfigures (b), (d), (f) show the trajectories of the substrate and biomass concentrations and dilution rate signal for $D_{max} = 1$. The limits of biomass concentrations are $(1/y_s)(s_{in} - s^*)$, $(1/y_s)s_{in}$.

Simulations of substrate and biomass concentrations show that (Figure 2):

i)   For each D_{max} value, the convergence region of the simulated s trajectory is inside the region bounded by the computed limit s^*, thus verifying the validity of theorem 3.1, and the residual set $\Omega_s = \{s : 0 < s \leq s^*\}$.

ii)   the substrate concentration s is outside the residual set Ω_s at initial time, it gets inside at 5.22 for D_{max}=1.65, and at 3.73 for $D_{max} = 1$, and it remains inside afterwards.

iii) For each D_{max} value, the convergence region of the simulated x trajectory is inside the region bounded by the computed limits $(1/y_s)(s_{in} - s^*)$, $(1/y_s)s_{in}$, thus verifying the validity of theorem 3.1, and the residual set $\Omega_x = \{x : (1/y_s)(s_{in} - s^*) \leq x < (1/y_s)s_{in}\}$.

Second simulation example. Continuous cultivation of *Gluconacetobacter diazotrophicus* is simulated, using conditions and data of batch cultivation with cane molasses as carbon source (see [69]), considering the Monod growth rate function:

$$\mu_s = \begin{cases} \mu_{mx} \dfrac{s}{k_s+s} - k_o & for \ \ s > k_s k_o/(\mu_{mx} - k_o) \\ 0 & for \ \ s \le k_s k_o/(\mu_{mx} - k_o) \end{cases} \tag{52}$$

Where $\mu_{mx} > k_o$.

The parameters of model (1) with this growth rate function were fitted to the batch data and are given in Table 1. For the growth rate function (52), the D_{max} value satisfies condition (30) and s^* is obtained from $\mu = D_{max}$:

$$\mu_{mx} \frac{s}{k_s + s} - k_o \bigg|_{s=s^*} = D_{max}$$

what leads to

$$s^* = \frac{(k_o + D_{max})k_s}{\mu_{mx} - k_o - D_{max}}$$

An example of D_{max}, s^* values is given in Table 1. The growth function (52), its main points, the gradient W (42) and Lyapunov function V_e (44) are illustrated in Figure 3.
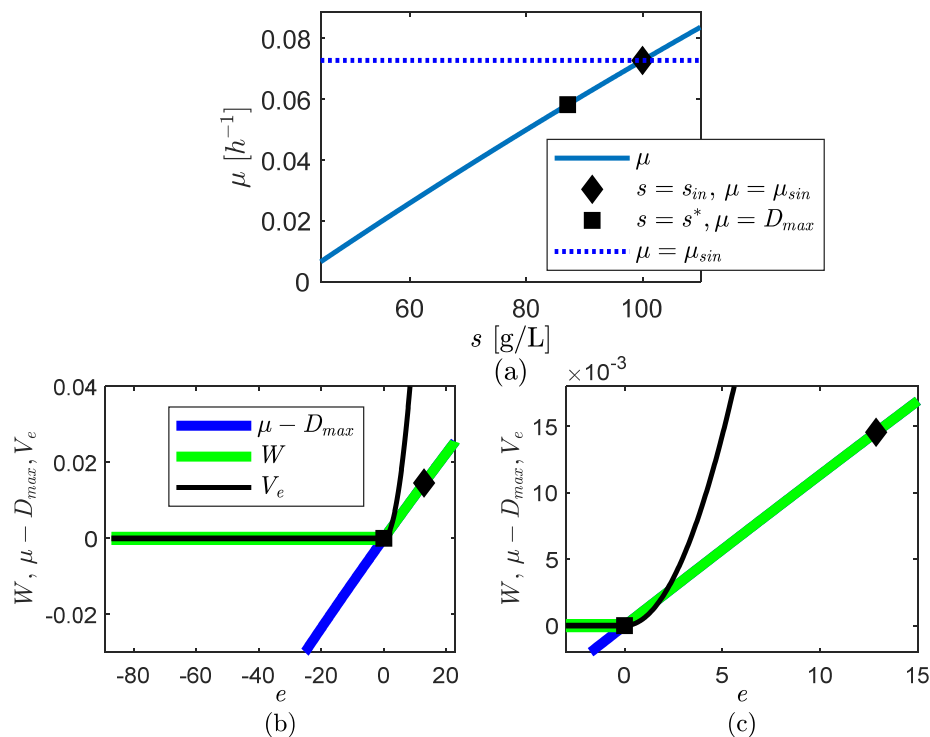

Figure 3. Monotonic growth rate function and its gradient: a) monotonic function (52); b) function $\mu - D_{max}$, gradient W and Lyapunov function V_e; c) detail of function $\mu - D_{max}$, gradient W and Lyapunov function V_e.

The time-varying dilution rate is:

$$D = \begin{cases} 0.5D_{max} + 0.5D_{max} sign\left(\sin\left(\frac{2\pi}{\tau_{d1}}t\right)\right) \quad for \quad t \in \Omega_{t1} \\ 0.5D_{max} + a_1 0.5D_{max} \sin\left(\frac{2\pi}{\tau_{d1}}t\right) + (1-a_1)0.5D_{max} \sin\left(\frac{2\pi}{\tau_{d2}}t\right) \quad otherwise \end{cases}$$

Where $a_1 = 0.9, \tau_{d1} = 120$ h, $\tau_{d2} = 120/9$ h and $\Omega_{t1} = [300, 550]$ h for $D_{max} = 0.0656$ h^{-1}; whereas $a_1 = 0.91$, $\tau_{d1} = 190$ h, $\tau_{d2} = 190/9$ h and $\Omega_{t1} = [350, 600]$ h for $D_{max} = 0.0291$ h^{-1}.
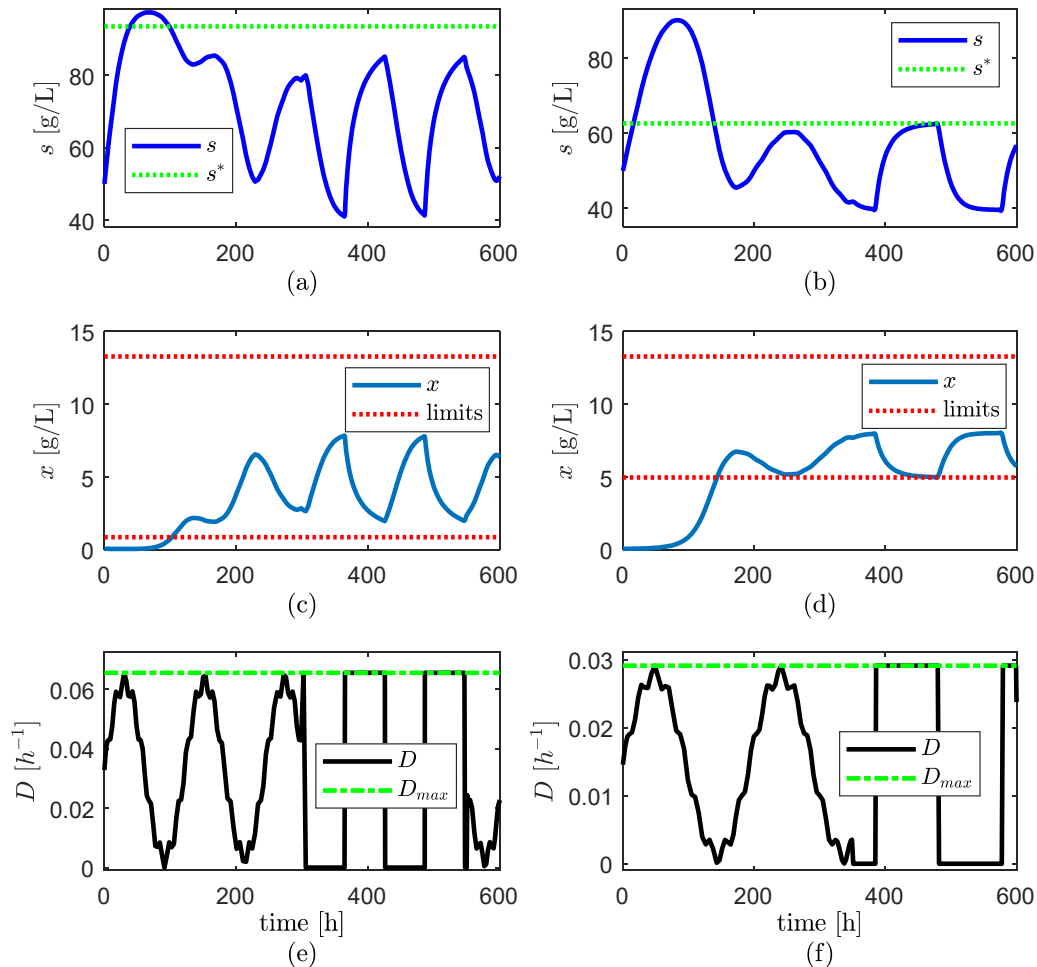
Figure 4. Simulation results for the second simulation example. Subfigures (a), (c), (e) show the trajectories of the substrate and biomass concentrations and dilution rate signal for $D_{max} = 0.0656$ h^{-1}. Subfigures (b), (d), (f) show the trajectories of the substrate and biomass concentrations and dilution rate signal for $D_{max} = 0.0291$ h^{-1}. The limits of biomass concentrations are $(1/y_s)(s_{in} - s^*)$, $(1/y_s)s_{in}$.

Simulations of substrate and biomass concentrations show that (Figure 4):

i) for each D_{max} value, the convergence region of the simulated s trajectory is inside the region bounded by the computed limit s^*, thus verifying the validity of theorem 3.2, and the residual set $\Omega_s = \{s: 0 < s \le s^*\}$.

ii) the substrate concentration s is inside the residual set Ω_s at the initial time, and it is outside only during $[40.7, 131.1]$ h for $D_{max} = 0.0656$ h^{-1} and during $[16.2, 138.7]$ h for $D_{max} = 0.0291$ h^{-1}.

iii) for each D_{max} value, the convergence region of the simulated x trajectory is inside the region bounded by the computed limits $(1/y_s)(s_{in} - s^*)$, $(1/y_s)s_{in}$, thus verifying the validity of Theorem 3.2, and the residual set $\Omega_x = \{x: (1/y_s)(s_{in} - s^*) \leq x < (1/y_s)s_{in}\}$.

General discussion on the numerical simulations. In summary, the first and second simulation examples show that the considered dilution rate constraint (9) and (29) with D_{max} conditions (10) and (30) leads to asymptotic convergence of the substrate concentration to the determined compact set $\Omega_s = \{s: 0 < s \leq s^*\}$ and asymptotic convergence of biomass concentration to the determined compact set $\Omega_x = \{x: (1/y_s)(s_{in} - s^*) \leq x < (1/y_s)s_{in}\}$, in presence of varying dilution rate within the defined set Ω_D. This illustrates Theorems 3.1 and 3.2, and verifies the validity of the residual sets $\Omega_s = \{s: 0 < s \leq s^*\}$, $\Omega_x = \{x: (1/y_s)(s_{in} - s^*) \leq x < (1/y_s)s_{in}\}$, where s^* is the solution of $\mu = D_{max}$ for $s = s^*$.

6. Conclusions

In this work, the global stability of a continuous bioreactor model is studied, with the concentrations of biomass and substrate as state variables. Non-monotonic and monotonic functions of substrate concentration are considered for the specific growth rate, whereas the dilution rate is time-varying but bounded, thus leading to state convergence to a compact set instead of an equilibrium point. Based on the Lyapunov function theory with dead-zone modification, the asymptotic convergence of the substrate and biomass concentrations is studied.

The main contributions with respect to closely related studies are: i) the convergence region of the substrate and biomass concentrations are determined as a function of the upper bound of the dilution rate (D), and the global asymptotic convergence to these compact sets is proved, considering monotonic and non-monotonic growth functions separately; ii) several improvements are proposed in the stability analysis, including the definition of a new dead zone Lyapunov function and the properties of its gradient. These improvements allow proving convergence of substrate and biomass concentrations to their compact sets, while tackling the interwoven and nonlinear nature of the dynamics of biomass and substrate concentrations, the non-monotonic nature of the specific growth rate, and the time-varying nature of the dilution rate. The proposed modifications are a basis for further global stability analysis of bioreactor models exhibiting convergence to a compact set instead of an equilibrium point. Finally, the convergence of the states and the biomass persistence under varying dilution rates are illustrated by simulation.

Conflict of interest

The authors declare that they have no conflict of interests.

References

1. T. Salmi, P. Tolvanen, K. Eränen, J. Wärnå, S. Leveneur, H. Haario, Determination of kinetic constants by using transient temperature data from continuous stirred tank reactors, *Chem. Eng. Sci.*, **248** (2022), 117164. https://doi.org/10.1016/j.ces.2021.117164

2. M. A. Siddiqui, Md. N. Anwar, S. H. Laskar, Control of nonlinear jacketed continuous stirred tank reactor using different control structures, *J. Process Control*, **108** (2021), 112–124. https://doi.org/10.1016/j.jprocont.2021.11.005

3. T. Caraballo, R. Colucci, J. López-de-la-Cruz, A. Rapaport, Study of the chemostat model with non-monotonic growth under random disturbances on the removal rate, *Math. Biosci. Eng.*, **17** (2020), 7480–7501. https://doi.org/10.3934/mbe.2020382

4. K. Bizon, B. Tabiś, Problems in volumetric flow rate and liquid level control of a continuous stirred tank bioreactor with structured and unstructured kinetics, *Chem. Eng. Res. Design*, **175** (2021), 309–319. https://doi.org/10.1016/j.cherd.2021.09.015

5. A. I. Bayu, R. A. Lestary, N. Dewayanto, M. Mellyanawaty, A. Wicaksono, R. W. Alvania-Kartika, et al., Kinetic study of thermophilic anaerobic digestion of sugarcane vinasse in a single-stage continuous stirred tank reactor, *Results Eng.*, **14** (2022), 100432. https://doi.org/10.1016/j.rineng.2022.100432

6. P. C. Ri, J. S. Kim, T. R. Kim, C. H. Pang, H. G. Mun, G. C. Pak, et al., Effect of hydraulic retention time on the hydrogen production in a horizontal and vertical continuous stirred-tank reactor, *Int. J. Hydrogen Energy*, **44** (2019), 17742–17749/ https://doi.org/10.1016/j.ijhydene.2019.05.136

7. J. Harmand, A. Rapaport, D. Dochain, Increasing the dilution rate can globally stabilize two-step biological systems, *J. Process Control*, **95** (2020), 67–74. https://doi.org/10.1016/j.jprocont.2020.08.009

8. H. de Battista, M. Jamilis, F. Garelli, J. Picó, Global stabilisation of continuous bioreactors: Tools for analysis and design of feeding laws, *Automatica*, **89** (2018), 340–348. https://doi.org/10.1016/j.automatica.2017.12.041

9. N. Dimitrova, P. Zlateva, Global stability analysis of a bioreactor model for phenol and cresol mixture degradation, *Processes*, **9** (2021), 124. https://doi.org/10.3390/pr9010124

10. L. Sridhar, Analysis of microalgae dynamics models, *Biofuels*, **11** (2020), 637–641. https://doi.org/10.1080/17597269.2017.1387747

11. F. Mairet, A. Rojas-Palma, Modeling and stability analysis of a microalgal pond with nitrification, *Appl. Math. Model*, **51** (2017), 448–468. https://doi.org/10.1016/j.apm.2017.07.008

12. M. Sbarciog, A. V. Wouwer, A constructive approach to assess the stability of anaerobic digestion systems, *Chem. Eng. Sci.*, **227** (2020), 115931. https://doi.org/10.1016/j.ces.2020.115931

13. P. Skupin, M. Metzger, Oscillatory behaviour control in a continuous culture under double-substrate limitation, *J. Biol. Dyn.*, **12** (2018), 663–682. https://doi.org/10.1080/17513758.2018.1502368

14. M. I. Nelson, H. S. Sidhu, Analysis of a chemostat model with variable yield coefficient, *J. Math. Chem.*, **38** (2005), 605–615. https://doi.org/10.1007/s10910-005-6914-2

15. J. Alvarez-Ramirez, J. Alvarez, A. Velasco, On the existence of sustained oscillations in a class of bioreactors, *Comput. Chem. Eng.*, **33** (2009), 4–9. https://doi.org/10.1016/j.compchemeng.2008.05.017

16. T. Sari, B. Benyahia, The operating diagram for a two-step anaerobic digestion model, *Nonlinear Dyn.*, **105** (2021), 2711–2737. https://doi.org/10.1007/s11071-021-06722-7

17. T. Sari, Best operating conditions for biogas production in some simple anaerobic digestion models, *Processes*, **10** (2022), 258. https://doi.org/10.3390/pr10020258

18. T. Meadows, M. Weedermann, G. S. K. Wolkowicz, Global analysis of a simplified model of anaerobic digestion and a new result for the chemostat, *SIAM J. Appl. Math.*, **79** (2019), 668–689. https://doi.org/10.1137/18M1198788

19. C. Martínez, J. L. Gouzé, Global dynamics of the chemostat with overflow metabolism, *J. Math. Biol.*, **82** (2021), 13. https://doi.org/10.1007/s00285-021-01566-6

20. R. Huang, Y. Wang, Global stability of a chemostat system with dispersal between multiple patches, *Nonlinear Dyn.*, **108** (2022), 4511–4529. https://doi.org/10.1007/s11071-022-07386-7

21. T. Sari, F. Mazenc, Global dynamics of the chemostat with different removal rates and variable yields, *Math. Biosci. Eng.*, **8** (2011), 827–840. https://doi.org/10.3934/mbe.2011.8.827

22. A. Rincón, G. Y. Florez, G. Olivar, Convergence assessment of the trajectories of a bioreaction system by using asymmetric truncated vertex functions, *Symmetry*, **12** (2020), 513. https://doi.org/10.3390/sym12040513

23. M. Dellal, B. Bar, Global analysis of a model of competition in the chemostat with internal inhibitor, *Discrete Contin. Dyn. Syst. B*, **26** (2021), 1129–1148. https://doi.org/10.3934/dcdsb.2020156

24. E. Ranjbar, M. Yaghubi, A. A. Suratgar, Robust adaptive sliding mode control of a MEMS tunable capacitor based on dead-zone method, *Automatika*, **61** (2020), 587–601. https://doi.org/10.1080/00051144.2020.1806011

25. Q. Hong, Y. Shi, Z. Chen, Dynamics modeling and tension control of composites winding system based on ASMC, *IEEE Access*, **8** (2020), 102795–102810. https://doi.org/10.1109/ACCESS.2020.2997340

26. A. Rincón, G. M. Restrepo, Ó. J. Sánchez, An improved robust adaptive controller for a fed-batch bioreactor with input saturation and unknown varying control gain via dead-zone quadratic forms, *Computation*, **9** (2021), 100. https://doi.org/10.3390/computation9090100

27. A. Rincón, G. M. Restrepo, F. E. Hoyos, A robust observer—based adaptive control of second—order systems with input saturation via dead-zone Lyapunov functions, *Computation*, **9** (2021), 82. https://doi.org/10.3390/computation9080082

28. S. Roy, S. Baldi, L. M. Fridman, On adaptive sliding mode control without a priori bounded uncertainty, *Automatica*, **111** (2020), 108650. https://doi.org/10.1016/j.automatica.2019.108650

29. Z. Ming, H. Zhang, Y. Liang, H. Su, Nonzero-sum differential games of continuous-time nonlinear systems with uniformly ultimately ε-bounded by adaptive dynamic programming, *Appl. Math. Comput.*, **430** (2022), 127248. https://doi.org/10.1016/j.amc.2022.127248

30. G. O. Tysse, A. Cibicik, L. Tingelstad, O. Egeland, Lyapunov-based damping controller with nonlinear MPC control of payload position for a knuckle boom crane, *Automatica*, **140** (2022), 110219. https://doi.org/10.1016/j.automatica.2022.110219

31. M. C. Valentino, F. A. Faria, V. A. Oliveira, L. F. C. Alberto, Sufficient conditions in terms of linear matrix inequalities for guaranteed ultimately boundedness of solutions of switched Takagi-Sugeno fuzzy systems using the s-procedure, *Inf. Sci.*, **572** (2021), 501–521. https://doi.org/10.1016/j.ins.2021.04.103

32. A. Boulkroune, M. M'saad, M. Farza, Adaptive fuzzy system-based variable-structure controller for multivariable nonaffine nonlinear uncertain systems subject to actuator nonlinearities, *Neural Comput. Appl.*, **28** (2017), 3371–3384. https://doi.org/10.1007/s00521-016-2241-8

33. M. Cai, Z. Xiang, Adaptive practical finite-time stabilization for uncertain nonstrict feedback nonlinear systems with input nonlinearity, *IEEE Trans. Syst. Man Cybern. Syst.*, **47** (2017), 1668–1678. https://doi.org/10.1109/TSMC.2017.2660761

34. E. Asiain, R. Garrido, Anti-chaos control of a servo system using nonlinear model reference adaptive control, *Chaos Solitons Fractals*, **143** (2021), 110581. https://doi.org/10.1016/j.chaos.2020.110581

35. W. Xue, M. Zhang, S. Liu, Y. Li, S. Cang, Mechanical analysis and ultimate boundary estimation of the chaotic permanent magnet synchronous motor, *J. Franklin Inst.*, **356** (2019), 5378–5394. https://doi.org/10.1016/j.jfranklin.2019.05.007

36. M. Fiaz, M. Aqeel, S. Ahmad, J. Ayub, The analysis of NSG system for existence of Si'lnikov chaos, *Chin. J. Phys.*, **62** (2019), 43–53. https://doi.org/10.1016/j.cjph.2019.09.013

37. F. Zhang, X. Liao, G. Zhang, C. Mu, Dynamical analysis of the generalized Lorenz systems, *J. Dyn. Control Syst.*, **23** (2017), 349–362. https://doi.org/10.1007/s10883-016-9325-8

38. X. Liao, G. Zhou, Q. Yang, Y. Fu, G. Chen, Constructive proof of Lagrange stability and sufficient—necessary conditions of Lyapunov stability for Yang—Chen chaotic system, *Appl. Math. Comput.*, **309** (2017), 205–221. https://doi.org/10.1016/j.amc.2017.03.033

39. S. Zeinali, M. Shahrokhi, Observer-based singularity free nonlinear controller for uncertain systems subject to input saturation, *Eur. J. Control*, **52** (2020), 49–58. https://doi.org/10.1016/j.ejcon.2019.08.001

40. J. Picó, H. de Battista, F. Garelli, Smooth sliding-mode observers for specific growth rate and substrate from biomass measurement, *J. Process Control*, **19** (2009), 1314–1323. https://doi.org/10.1016/j.jprocont.2009.04.001

41. G. Bastin, D. Dochain, *On-Line Estimation and Adaptive Control of Bioreactors*, Elsevier, 1990.

42. A. Rapaport, T. Nidelet, S. El-Aida, J. Harmand, About biomass overyielding of mixed cultures in batch processes, *Math. Biosci.*, **322** (2020), 108322. https://doi.org/10.1016/j.mbs.2020.108322

43. J. L. Gouzé, G. Robledo, Feedback control for nonmonotone competition models in the chemostat, *Nonlinear Anal. Real World Appl.*, **6** (2005), 671–690. https://doi.org/10.1016/j.nonrwa.2004.12.003

44. G. J. Butler, G. S. K. Wolkowicz, A mathematical model of the chemostat with a general class of functions describing nutrient uptake, *SIAM J. Appl. Math.*, **45** (1985), 138–151. https://doi.org/10.1137/0145006

45. F. Mazenc, M. Malisoff, Stabilization of a chemostat model with Haldane growth functions and a delay in the measurements, *Automatica*, **46** (2010), 1428–1436. https://doi.org/10.1016/j.automatica.2010.06.012

46. J. H. T. Luong, Generalization of Monod kinetics for analysis of growth data with substrate inhibition, *Biotechnol. Bioeng.*, **29** (1987), 242–248. https://doi.org/10.1002/bit.260290215

47. S. K. C. Lin, C. Du, A. Koutinas, R. Wang, C. Webb, Substrate and product inhibition kinetics in succinic acid production by Actinobacillus succinogenes, *Biochem. Eng. J.*, **41** (2008), 128–135. https://doi.org/10.1016/j.bej.2008.03.013

48. J. F. Andrews, A mathematical model for the continuous culture of microorganisms utilizing inhibitory substrates, *Biotechnol. Bioeng.*, **10** (1968), 707–723. https://doi.org/10.1002/bit.260100602

49. O. Bernard, Z. Hadj-Sadok, D. Dochain, A. Genovesi, J. P. Steyer, Dynamical model development and parameter identification for an anaerobic wastewater treatment process, *Biotechnol. Bioeng.*, **75** (2001), 424–438. https://doi.org/10.1002/bit.10036

50. J. Ribes, K. Keesman, H. Spanjers, Modelling anaerobic biomass growth kinetics with a substrate threshold concentration, *Water Res.*, **38** (2004), 4502–4510. https://doi.org/10.1016/j.watres.2004.08.017

51. J. Slotine; W. Li, *Applied Nonlinear Control*, Englewood Cliffs, 1991.

52. K. M. Koo, Stable adaptive fuzzy controller with time-varying dead-zone, *Fuzzy Sets Syst.*, **121** (2001), 161–168. https://doi.org/10.1016/S0165-0114(99)00157-8

53. X. S. Wang, C. Y. Su, H. Hong, Robust adaptive control of a class of nonlinear systems with unknown dead-zone, *Automatica*, **40** (2004), 407–413. https://doi.org/10.1016/j.automatica.2003.10.021

54. P. Ioannou, J. Sun, *Robust Adaptive Control*, Prentice-Hall PTR, 1996.

55. E. D. Sontag, Y. Wang, On characterizations of the input-to-state stability property, *Syst. Control Lett.*, **24** (1995), 351–359. https://doi.org/10.1016/0167-6911(94)00050-6

56. A. Rincón, J. Villa, F. Angulo, G. Olivar, A dynamic analysis for an anaerobic digester: Stability and bifurcation branches, *Math. Probl. Eng.*, **2014** (2014), 1–14. https://doi.org/10.1155/2014/514797

57. Y. A. Kuznetsov, *Elements of Applied Bifurcation Theory*, Springer, **112** (2004).

58. M. Sbarciog, M. Loccufier, E. Noldus, Convergence and stability of biochemical reaction systems of rank one, in *Proceedings of the Proceedings of the 44th IEEE Conference on Decision and Control*, (2005), 5540–5545. https://doi.org/10.1109/CDC.2005.1583044

59. J. Hess, O. Bernard, Design and study of a risk management criterion for an unstable anaerobic wastewater treatment process, *J. Process Control*, **18** (2008), 71–79. https://doi.org/10.1016/j.jprocont.2007.05.005

60. B. Haegeman, A. Rapaport, How flocculation can explain coexistence in the chemostat, *J. Biol. Dyn.*, **2** (2008), 1–13. https://doi.org/10.1080/17513750801942537

61. I. R. Moyles, J. G. Donohue, A. C. Fowler, Quasi-steady uptake and bacterial community assembly in a mathematical model of soil-phosphorus mobility, *J. Theor. Biol.*, **509** (2021), 110530. https://doi.org/10.1016/j.jtbi.2020.110530

62. I. R. Moyles, A. C. Fowler, Production of nitrate spikes in a model of ammonium biodegradation, *Theor. Ecol.*, **11** (2018), 333–350. https://doi.org/10.1007/s12080-018-0370-7

63. M. J. McGuinness, L. B. Cribbin, H. F. Winstanley, A. C. Fowler, Modelling spatial oscillations in soil borehole bacteria, *J. Theor. Biol.*, **363** (2014), 74–79. https://doi.org/10.1016/j.jtbi.2014.08.017

64. A. C. Fowler, H. F. Winstanley, M. J. McGuinness, L. B. Cribbin, Oscillations in soil bacterial redox reactions, *J. Theor. Biol.*, 2014, **342** (2014), 33–38. https://doi.org/10.1016/j.jtbi.2013.10.010

65. H. Zhang, Y. Cai, S. Fu, W. Wang, Impact of the fear effect in a prey-predator model incorporating a prey refuge, *Appl. Math. Comput.*, 2019, **356** (2019), 328–337. https://doi.org/10.1016/j.amc.2019.03.034

66. Z. Shang, Y. Qiao, L. Duan, J. Miao, Bifurcation analysis and global dynamics in a predator–prey system of Leslie type with an increasing functional response, *Ecol. Modell.*, **455** (2021), 109660. https://doi.org/10.1016/j.ecolmodel.2021.109660

67. S. B. Hsu, A survey of constructing Lyapunov functions for mathematical models in population biology, *Taiwan. J. Math.*, **9** (2005), https://doi.org/10.11650/twjm/1500407791

68. X. Gan, H. Wang, P. Ao, Existence of a smooth Lyapunov function for any smooth planar dynamical system with one limit cycle, *Nonlinear Dyn.*, **105** (2021), 3117–3130. https://doi.org/10.1007/s11071-021-06775-8

69. A. Rincón-Santamaría, J. A. Cuellar-Gil, L. F. Valencia-Gil, O. J. Sánchez-Toro, Cinética de Crecimiento de Gluconacetobacter Diazotrophicus Usando Melaza de Caña y Sacarosa: Evaluación de Modelos, *Acta Biol. Colomb.*, **24** (2019), 38–57. https://doi.org/10.15446/abc.v24n1.70857

Appendix

Proof of Eq (22).
From the W properties (14) or alternatively from the definition of W (20) it follows that

$$W > 0 \quad for \quad s > s^* \tag{A1}$$

From property (19) and the W definition (20) it follows that

$$\mu - D_{max} \geq W \quad for \; s > s^*$$

Combining with properties (18), (14), yields

$$0 < W \leq \mu - D_{max} \leq \mu - D, \quad for \; s > s^*$$

That is,

$$\mu - D \geq W > 0 \quad for \; s > s^*$$

Combining with result (A1), yields

$$W(\mu - D) \geq W^2 > 0 \; for \; s > s^* \tag{A2}$$

From the W definition (20) and properties (14) it follows that

$$W(\mu - D) = 0 = W^2 \quad for \; s \leq s^*$$

Combining with Eq (A2), yields

$$W(\mu - D) \geq W^2 \geq 0$$

This completes the proof.